Point-geometry angular correlation curves for Cu: A study of enhancement in positron annihilation

P. E. Mijnarends
Netherlands Energy Research Foundation ECN, 1755 ZG Petten (N.H.), The Netherlands

R. M. Singru*
Institut für Festkörperforschung, Kernforschungsanlage Jülich, 5170 Jülich, Federal Republic of Germany
(Received 23 October 1978; revised manuscript received 30 January 1979)

New band-structure calculations of point-slit angular correlation curves for positron annihilation in Cu single crystals are compared with measurements by Mader and Berko *et al.* Corrections are applied for the geometrical resolution and for enhancement due to e^--e^- and e^+-e^- correlations. A new energy-dependent form of "Kahana enhancement" is proposed that gives excellent agreement between theory and experiment if the core contribution is reduced by a factor of 5. The results qualitatively confirm the enhancement of umklapp contributions derived by Hede and Carbotte. No indication is found for a de-enhancement of the umklapp components proposed by Fujiwara *et al.* Calculated curves for α-$Cu_{0.7}Zn_{0.3}$ obtained on the basis of a rigid-band model are given for future reference.

I. INTRODUCTION

In recent years measurements of the angular correlation between the quanta from the annihilation of thermalized positrons have been used to study the Fermi surface and the two-photon momentum density in a large number of metals and alloys.[1-4] As known, the latter quantity is closely related to the electron momentum density. Most of the measurements have been done with the conventional long-slit geometry which resolves only one of the three momentum components. However, the recent development of two-dimensional angular correlation machines[2,5-9] that simultaneously measure two momentum components allows these studies to be carried out in much greater detail. On the theoretical side there has been considerable progress in calculating the two-photon momentum density in solids employing different band-structure methods. In many cases a fairly satisfactory agreement has been reached between theory and experiment using the long-slit geometry.[10-12] Calculations of two-dimensional angular correlation curves are of more recent date but can in combination with corresponding measurements provide far more detailed information than their long-slit counterparts. A good example of such a study is the recent work on aluminum by Mader *et al.*[13] where the umklapp components (for which $\vec{p}=\vec{k}+\vec{G}$ with $\vec{G}$ a vector of the reciprocal lattice[14]) could be studied without interference from the intense low-momentum part of the momentum distribution. This study also provided valuable information on the conduction- and core-electron enhancement due to many-body effects. This latter aspect is of even greater interest in *d*-band metals with their complicated band structure and strongly anisotropic momentum density.

Kahana[15] has discussed the theory of enhancement for a positron in a free-electron gas. He describes the enhancement by a factor

$$\epsilon(p)=a+b(p/p_F)^2+c(p/p_F)^4, \quad p<p_F, \tag{1}$$

multiplying the independent-particle two-photon momentum density. Here a, b, and c are constants depending on the electron density and p_F is the free-electron Fermi momentum. When the enhancement factor is integrated over the volume enclosed by the Fermi surface it is able, after appropriate correction for the core contribution, to explain the observed positron lifetimes in simple metals, which are an order of magnitude shorter than one would expect from independent-particle theory. At the same time, the momentum density is only little affected (apart from a scale factor). Other authors have performed model calculations of the enhancement in the presence of a (weak) lattice potential. Hede and Carbotte[16] have considered the enhancement of the umklapp components in a nearly-free-electron (NFE) system. Their calculations yield an enhancement of the umklapp contribution that is approximately constant and somewhat lower than that for the central free-electron parabola, but slightly increasing towards the edge of the umklapp Fermi sphere. Fujiwara and co-workers[17] have discussed the enhancement effects due to intraband and interband electron transitions in a two-band NFE model. They conclude that near a zone face the intraband transitions produce an enhancement factor qualitatively similar to that derived by Kahana, while the interband transitions of electrons from

the lower to the upper band cause a reduction ("de-enhancement") of the umklapp components.

So far, no prescription of how to correct for enhancement in cases of practical interest has emerged from these lattice theories and the theory of Kahana is the only one that has found widespread practical application in simple metals. In Na,[18] Li,[19] and Al,[13] it produces the characteristic bulge found experimentally at momenta $p < p_F$. Its usefulness in d-band metals is questionable, however. The hybridization between the conduction and d bands in these metals causes the Fermi surface to be anisotropic and poses the problem whether the enhancement correction should be applied to conduction and d electrons alike or only to the former. In the first case the d bands are far from parabolic and Eq. (1) cannot be expected to hold, while in the latter case the question arises how to separate the hybridized conduction and d bands.

The tightly bound core electrons will also correlate with the positron, but the ensuing enhancement will be smaller than that for the band electrons since they are less free to move. According to a calculation by Carbotte and Salvadori[20] the core enhancement is a nearly p-independent scaling factor of ~3.6 for Na and ~2.8 for Al.

Recently, measurements of the two-dimensional angular correlations in copper have been performed by Mader[21] and Berko *et al.*[5,22] In the present paper we intend to approach the question of enhancement in d-band metals from the experimental side. We report a band-structure calculation of the two-photon momentum density and some two-dimensional angular correlation curves for copper and compare the results with the data of Mader and Berko *et al.* Copper is an ideal test case for a variety of reasons. First, its band structure and Fermi surface are well understood, both experimentally and theoretically. Second, its Fermi surface consists of only one (multiply connected) sheet, thereby avoiding the complications inherent in the multiple-sheet Fermi surfaces found in transition metals. Third, extensive positron annihilation studies have been performed on copper single crystals with different slit geometries (see the references cited in Ref. 4), and, finally, copper forms many alloys which enable one to conveniently vary the electron density in future enhancement studies.

In the present calculations the effect of enhancement is included in two different ways. The first one consists of straightforward application of Eq. (1). Detailed comparison with the experimental data, however, shows that better results are obtained if Kahana's prescription is transcribed in an energy-dependent form that we propose in Sec. II of this paper. Particular attention is given to the neck region of the Fermi surface where this comparison allows us to test the current ideas about enhancement near a zone face. As an extension of this work, two-dimensional angular correlation curves for the alloy α-$Cu_{0.7}Zn_{0.3}$ have been calculated in the rigid-band approximation for future reference. Recent calculations by Bansil *et al.*[23] employing the average-t-matrix approximation (ATA) and positron annihilation measurements[24] of Fermi-surface radii have shown that as Zn is added to Cu the swelling of the Fermi surface follows the predictions of the rigid-band model reasonably closely. Furthermore, it has appeared from previous work on $3d$ metals[25] that the partial electron momentum densities due to the individual bands do not change much in going from one metal to the next higher one with the same crystal structure (e.g., from fcc Ni to fcc Cu). Differences between the total momentum densities in these metals derive mainly from the change in position of the Fermi level. This suggests that as long as detailed ATA or coherent-potential-approximation (CPA) calculations of the two-quantum momentum density in disordered alloys are not available[26,27] for comparison with experiment, the rigid-band model may constitute a useful first approximation. It should be stressed, however, that this model does not describe the damping of the Bloch states due to the disorder in the alloy.

The plan of the present paper is as follows. The details of the calculations are given in Sec. II, while in Sec. III the results are presented and compared with experiment. A general discussion of the results in Sec. IV concludes the paper.

II. CALCULATIONS

As known, the two-photon momentum density $\rho_b(\vec{p})$ due to the $3d$ and conduction electrons may be obtained from

$$\rho_b(\vec{p}) = \text{const} \sum_{\text{occ}\,\vec{k},j} |A_j(\vec{p},\vec{k})|^2 \delta(\vec{p}-\vec{k}-\vec{G}), \qquad (2)$$

with

$$A_j(\vec{p},\vec{k}) = \int_{\text{cell}} \exp(-i\vec{p}\cdot\vec{r})\,\psi_{\vec{k},j}(\vec{r})\,\phi_+(\vec{r})\,d\vec{r}. \qquad (3)$$

Here $\psi_{\vec{k},j}(\vec{r})$ denotes the Bloch wave function of the electron with wave vector $\vec{k}$ in the jth band and $\phi_+(\vec{r})$ the positron ground-state wave function. The summation in Eq. (2) is restricted to states below the Fermi level E_F. The present calculations were based on the muffin-tin potential of Chodorow. This potential is known to give a satisfactory description of the band structure of copper.[28] The method employed to calculate the band structure and the two-photon momentum density $\rho_b(\vec{p})$ from

TABLE I. Crystal orientations $\{p_z, p_x\}$ and mesh used for the calculated angular correlations.

Angular correlation symbol	p_z, p_x $p_y = 0$	Plane	Mesh[a] $\Delta p_z \times \Delta p_x$
A	[001], [100]	(010)	0.84×0.84
B	[001], [110]	($\bar{1}$10)	0.84×1.19
C	[101], [10$\bar{1}$]	(010)	0.59×1.19
D	[111], [$\bar{1}$10]	($\bar{1}\bar{1}$2)	0.97×1.19

[a] In units of $mc \times 10^{-3}$ (Ref. 40).

this potential is based on Hubbard's approximation scheme.[29] Details of this method may be found in earlier reports on Fe,[30] Cu,[30] and Ni.[12] In Hubbard's original formulation a set of four "preferred" reciprocal-lattice vectors is used, giving rise to a secular equation of minimal size but also to a slight lack of symmetry in the wave functions. In the present work this has been avoided by extending the preferred set to include the first two complete shells, i.e., a total of 15 vectors. Outside the muffin-tin sphere of radius $r_i = 2.4151$ a.u. the wave functions have been expanded in 113 plane waves. The same potential (apart from a minus sign) and the same number of plane waves have been used to describe the positron wave function.[31] The lattice constant used is 6.83087 a.u.

The momentum density $\rho_b(\vec{p})$ of the band electrons was calculated in the (010), ($\bar{1}$10), and ($\bar{1}\bar{1}$2) planes on meshes given in Table I. Numerical tests show that these meshes provide angular correlation curves that converge to within 0.3%. The contribution $\rho_c(\vec{p})$ from the core electrons was calculated in the spherical approximation[12] employing free-atom wave functions.[32] These results were used to calculate the two-dimensional angular correlation curves according to

$$N(p_y, p_z) = \int \rho(p_x, p_y, p_z)\, dp_x , \tag{4}$$

where $\rho(\vec{p})$ denotes the total momentum density. In order to display a possible structure in the curves more clearly the derivatives of the experimental and calculated angular correlation curves have also been calculated. For the experimental curves this has been done by locally performing a weighted least-squares fit of a third-degree polynomial to five data points and calculating the derivative to this polynomial, thus introducing a small amount of smoothing. Polynomials orthogonal over the set of five points have been used[33] to avoid the instabilities inherent in the use of ordinary power series, while the error bars have been computed from the statistical errors of the points participating in the fit.[34] The calculated curves have been differentiated with the aid of third-degree orthogonal polynomials fitted to four points.

A. Resolution

Before comparing the calculated curves with the experimental data a correction must be applied for the angular resolution of the setup. The easiest way to do this is by folding the theoretical curves with the p_y and p_z resolution functions. These can be approximated by Gaussians with a full width at half maximum (w_{FWHM}) of 2.8 and 0.609 mrad, respectively.[21,35] The folding is performed by $(2n+1)$-point Hermite-Gauss quadrature following[36]

$$F(p) = (\lambda/\pi^{1/2}) \int_{-\infty}^{\infty} \exp(-\lambda^2 t^2) f(p+t)\, dt$$

$$\sim \sum_{i=-n}^{n} c_i f(p + q_i/\lambda), \tag{5}$$

with $\lambda = 2(\ln 2)^{1/2}/(w_{\mathrm{FWHM}})$. The correction for the p_y resolution required the calculation of $\rho(\vec{p})$ in planes parallel to the selected plane $p_y = \text{const}$ and was performed by both three- and five-point quadrature. The p_z resolution was folded in with the aid of the five-point formula. The values of c_i and q_i are listed in Table II.

B. Enhancement

The principal goal of the present work was to study the enhancement due to the combined $e^- - e^-$ and $e^- - e^+$ correlations. As already mentioned, Eq. (1) can only be expected to give reasonable results when applied to an approximately parabolic conduction band. Its functional dependence on p/p_F then ensures that the enhancement $\epsilon(p)$ is

TABLE II. Coefficients c_i and abcissae q_i for use in three- and five-point Hermite-Gauss quadrature (after Ref. 36).

three-point	$c_0 = 0.666\,667$	$q_0 = 0$
	$c_{\pm 1} = 0.166\,667$	$q_{\pm 1} = \pm 1.224\,745$
five-point	$c_0 = 0.533\,333$	$q_0 = 0$
	$c_{\pm 1} = 0.222\,076$	$q_{\pm 1} = \pm 0.958\,572$
	$c_{\pm 2} = 0.011\,257$	$q_{\pm 2} = \pm 2.020\,183$

greatest for electrons close to the Fermi surface. These are the ones that are most free to correlate with the positron.

If one attempts to apply this correction to a d-band metal a number of problems arise. The hybridization between conduction and d bands prevents an unambiguous separation between the corresponding groups of electrons. One could consider applying Eq. (1) within the first Brillouin zone to all occupied conduction and d states alike, but this procedure would be manifestly incorrect. The d states close to the zone boundary in the lowest band would be enhanced by a large factor although in energy they are far removed from the Fermi level. Angular correlation curves calculated by us with this form of enhancement[37] showed a large bulge at values of p_z a little greater than the Fermi cutoff, in disagreement with experiment. This bulge can be removed by restricting the application of the enhancement correction to conduction and d states with momenta smaller than the Fermi momentum $|\vec{p}_F|$. Although the resulting angular correlation curves compare reasonably well with the experimental curves, the artificiality of this procedure, in which part of a filled band is enhanced and another part of that same band (i.e., the states with $|\vec{k}| > |\vec{p}_F|$) is not, is obvious. That this procedure nevertheless yields reasonable results can be explained by the fact that the d-electron contribution to $\rho(\vec{p})$ peaks in the outer part of the first zone. In the inner region it is relatively small and thus enhancement of this d contribution does not have much effect on the total momentum density. Yet, the overall conclusion must be that writing the enhancement factor as some functional of p does not allow a simple and natural extension of the enhancement correction to d bands.

However, a slightly different approach proves more fruitful. For a NFE gas with a quadratic dispersion law, Eq. (1) can also be written as a functional of energy rather than momentum:

$$\epsilon'(E) = a + b(E/E_F) + c(E/E_F)^2 , \tag{6}$$

where E and E_F are both counted from the bottom of the conduction band. For a quadratic conduction band Eq. (6) is identical to Eq. (1), but it can be extended in a natural way to d states by substituting for E the actual dispersion relations $E_j(\vec{k})$. Moreover, it possesses the attractive feature that ϵ' now depends on the distance in energy from the Fermi level. Low-lying d states are little enhanced while d states near E_F undergo the same enhancement as conduction states of equal energy. We therefore propose Eq. (6) as a purely empirical prescription for the enhancement correction. In the present study this form has been used with the values[37] for b/a and c/a originally prescribed by Kahana[15] for use in Eq. (1) and with a set to unity. The latter choice implies that all states outside the first Brillouin zone are in fact enhanced by a factor $\epsilon'(\Gamma_1)$ corresponding to the Γ_1 state at $\vec{k}=0$, while the enhancement of the core states, being less than $\epsilon'(\Gamma_1)$, is described by a core reduction factor α times $\epsilon'(\Gamma_1)$ (see below). This procedure is justified since in an angular correlation measurement only the *shape* of the curve is measured. It yields excellent results provided that the enhancement Eq. (6) is restricted to the first Brillouin zone. An attempt to apply Eq. (6) throughout all of $\vec{p}$ space, thereby mimicking the enhancement of the umklapp contributions proposed by Hede and Carbotte,[16] gave rise to relatively large bulges at momenta corresponding to the umklapp components and to a general overestimate of the high-momentum part of the curves, and was therefore abandoned.

C. Fraction of core annihilations

The study of Al by Mader *et al.*[13] has shown that a reasonable agreement between theory and experiment could only be obtained after reduction of the calculated core distribution by a factor of 2 with respect to the (enhanced) conduction electrons. Physically this reflects the smaller polarizability of the tightly bound core electrons. A similar core reduction factor α, adjustable between unity and zero, has been employed in the present work. It is the only fitting parameter in this work.

D. Statistical test

In view of the large number of calculations required to investigate the influence of different forms of enhancement, fraction of core annihilation, resolution, etc., for a number of crystal orientations it is impossible to present the comparison between theory and experiment for all these cases in a graphical form. Furthermore, the overall agreement is so good that the eye is not sensitive enough to detect small improvements in the fits. A χ^2 test enables one to characterize the quality of a fit by one single number.[38] If the number of data points $k>30$ and the calculated and measured curves represent the same distribution, then

$$\hat{\sigma} = (2\chi^2)^{1/2} - (2k-1)^{1/2} \tag{7}$$

is normally distributed with zero mean and variance unity. $\hat{\sigma}$ thus serves as a goodness-of-fit parameter. The probability that $\hat{\sigma}>1$, 2, 3, or 5 is 0.16, 0.023, 0.0013, or 2.9×10^{-7}, respectively.

III. RESULTS

A. Band structure and momentum density

The present band structure is in good agreement with that reported by Burdick.[28] The rms difference of 150 levels between −0.1 and 1.1 Ry (all energies with respect to the muffin-tin zero) is 5.7 mRy with relatively large contributions from two levels above 1 Ry. On the average, the present levels are shifted upward by about 3 mRy with respect to Burdick's. However, a check of a number of levels with the aid of a Korringa-Kohn-Rostoker (KKR) program reproduced the present values (to within about 1 mRy) rather than Burdick's. The actual error is therefore expected to be rather less than the value of 5.7 mRy quoted above.

A comparison of the dimensions of the Fermi surface (FS) constructed by Burdick with those of the "Cu7" surface obtained by Halse[39] from measurements of the de Haas–van Alphen effect shows that the former is smaller by an amount varying from 1.8% for k_{100} to 0.4% for k_{110}. In view of this and the systematic upward shift already mentioned we have raised the Fermi level from Burdick's value of 0.555 Ry to 0.562 Ry. This yielded a FS of the correct volume and slightly less anisotropic than the experimental one ($\Delta k_{100} = -1.1\%$, $\Delta k_{110} = +0.3\%$ with respect to Halse). The FS geometry obtained by us in the (010) and ($1\bar{1}0$) planes is shown in Fig. 1. The positron energy was found to be 0.559 Ry with respect to the positron muffin-tin zero which equals the electron muffin-tin zero apart from sign reversal.

Some representative results for the momentum density $\rho_b(\vec{p})$ due to the band electrons are shown

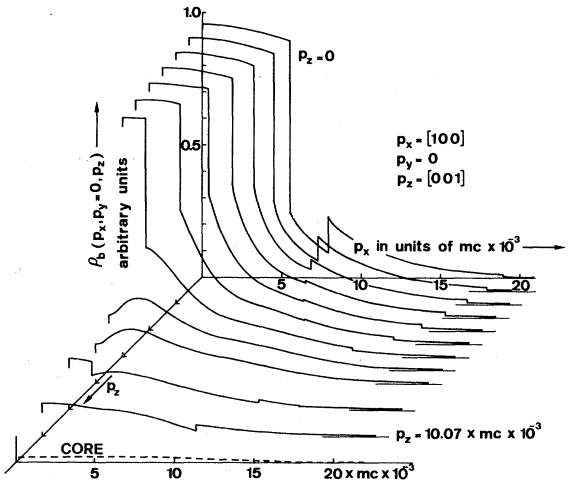

FIG. 2. Two-photon momentum density $\rho_b(p_x, p_y = 0, p_z)$ vs p_x in the (010) plane for Cu for different values of p_z (see text). The ticks along the p_z axis mark intervals of $1.68 \times mc \times 10^{-3}$. The dashed curve represents the core contribution ρ_c at $p_z = 0$.

in Figs. 2 and 3 where graphs of $\rho_b(p_x, p_y = 0, p_z)$ vs p_x for $p_z = 0.0$, 0.84, 1.68, 2.52, 3.36, 4.20, 5.04, 5.87, 6.71, 8.39, and $10.07 \times mc \times 10^{-3}$ are shown.[40] The dashed curve in Fig. 2 describes the isotropic core contribution at $p_z = 0$ (with unit weight). These results are similar to those reported earlier[30] for the ⟨100⟩, ⟨110⟩, and ⟨111⟩ directions and provide an additional insight into the anisotropic behavior of $\rho_b(\vec{p})$ in copper. The curves, when examined in conjunction with the FS geometry in Fig. 1, clearly bring out the effect of the FS discontinuities and the overlap integral $|A_j(\vec{p}, \vec{k})|^2$ on the momentum density. Detailed dis-

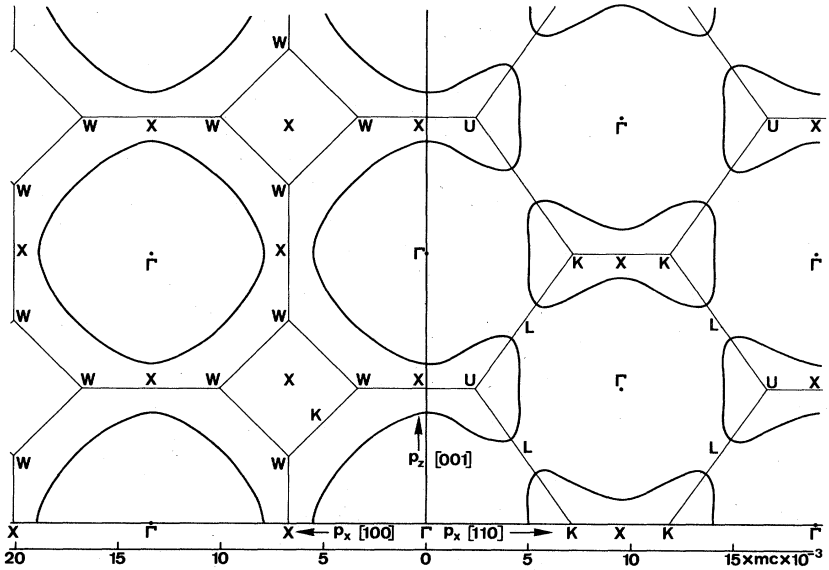

FIG. 1. Fermi surface of Cu in the (010) and ($1\bar{1}0$) planes in the extended zone scheme.

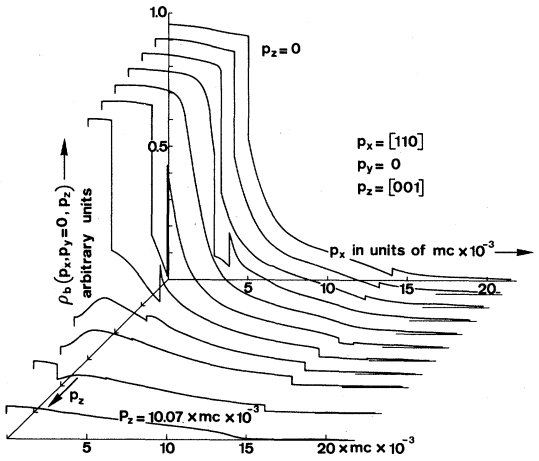

FIG. 3. As Fig. 2, but for the $(1\bar{1}0)$ plane.

cussions of the band-structure effects on $\rho_b(\vec{p})$ can be found elsewhere.[12,25,30]

B. Two-dimensional angular correlations

1. Copper

Two-dimensional angular correlations have been calculated for the orientations listed in Table I. In order to facilitate comparison with the experimental data,[21,22] all calculated and measured curves have been normalized to unit area under the curve (with p_z expressed in atomic units[40]). Since the experimental curves have only been measured up to ~20 mrad they have been extrapolated exponentially prior to normalization. As discussed earlier, the theoretical curves consist of a band and a core-electron contribution. The band contribution is calculated without enhancement correction and with enhancement according to Eq. (1) (p dependent) and Eq. (6) (E dependent).[37] For each of these we vary the core fraction α between 1.0 and 0.1. Moreover, we investigate the influence of the FS shape and of the way in which the p_y resolution correction is applied. Table III shows the good-

TABLE III. Values of the goodness-of-fit parameter $\hat{\sigma}$ for various combinations of the parameters.

Orient.	FS geom.[a]	Enhancement	p_y resol.[b]	Core fraction α 1.0	0.7	0.5	0.4	0.3	0.2	0.1
A	bs	no	five-point	59.4	46.5	38.0	34.0	30.0	26.4	23.2
B				53.2	43.2	36.8	33.7	30.8	28.1	25.7
C				28.2	22.8	19.4	17.7	16.1	14.7	13.4
D				77.1	60.4	49.7	44.6	39.9	35.7	32.2
A	Ha	Eq. (1)	five-point	29.0	19.4	15.4	14.7	15.1	16.5	18.9
B				29.9	24.4	22.7	22.7	23.2	24.2	25.9
C				13.0	10.7	10.3	10.5	11.0	11.7	12.7
D				39.2	29.2	26.5	26.9	28.5	31.3	35.1
A	Ha	Eq. (6)	no	43.8	36.1	32.8	31.8	31.5	31.8	32.7
B				26.5	27.5	30.3	32.4	34.8	37.5	40.6
C				10.4	6.0	3.9	3.2	2.9	3.0	3.5
D				83.7	76.0	72.8	71.9	71.4	71.6	72.3
A	bs	Eq. (6)	five-point	32.6	20.8	14.2	11.7	10.2	9.9	11.0
B				22.3	14.0	10.4	9.7	9.9	11.0	13.0
C				11.3	6.6	4.1	3.3	2.8	2.7	3.0
D				44.7	32.8	28.1	27.3	27.7	29.3	32.1
A	Ha	Eq. (6)	three-point	33.1	21.6	15.2	12.9	11.6	11.4	12.4
B				19.9	12.3	9.9	9.8	10.7	12.5	15.0
C				11.4	6.9	4.5	3.8	3.3	3.3	3.6
A	Ha	Eq. (6)	five-point	32.5	20.8	14.1	11.7	10.1	9.9	10.9
B				22.5	14.2	10.7	9.9	10.1	11.2	13.2
C				11.0	6.3	4.0	3.2	2.7	2.7	3.0
D				43.8	33.0	29.2	28.9	29.7	31.7	34.8
A	Ha	Eq. (6)	five-point	32.9[c]	21.1	14.0	11.0	8.9	7.9	8.3
B				22.3[c]	14.4	10.8	9.9	9.8	10.6	12.1
C				11.3[c]	6.6	4.2	3.27	2.69	2.48	2.69
D				45.3[c]	30.8	22.5	19.3	17.1	16.3	17.0

[a] bs: FS geometry from this band-structure calculation; Ha: Halse Cu7 FS (Ref. 39).
[b] Three-point (five-point) Hermite-Gauss quadrature.
[c] Values in this row calculated under exclusion of data points just beyond the zone boundary (see text).

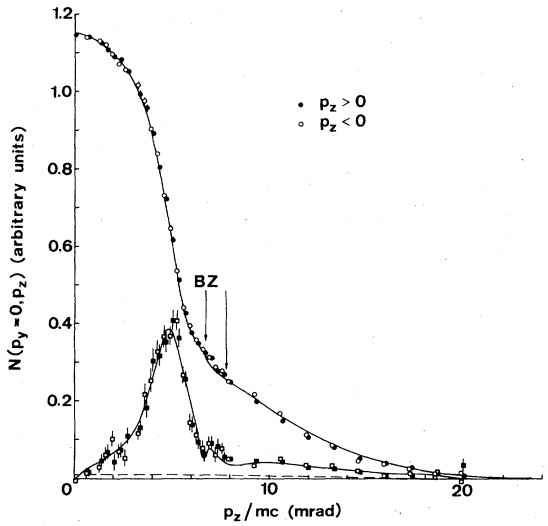

FIG. 4. Calculated point-slit angular correlation curve and derivative for orientation A ($\{p_z,p_x\}=\{[001],[100]\}$). Experimental points by Mader (Ref. 21) and Berko *et al.* (unpublished). Unless shown differently, error bars are smaller than the diameter of the points. Dashed curve: core contribution multiplied by core fraction α. Arrows indicate the interval excluded from $\hat{\sigma}$ in Row 7 of Table III. BZ: Brillouin-zone boundary.

ness-of-fit parameter $\hat{\sigma}$ for some of the calculations.

Rows 6 and 7 in Table III clearly show the great improvement obtained by the application of the energy-dependent enhancement correction Eq. (6) in comparison with both the unenhanced results (row 1) and the p-dependent enhancement (row 2) (the difference between rows 6 and 7 is explained

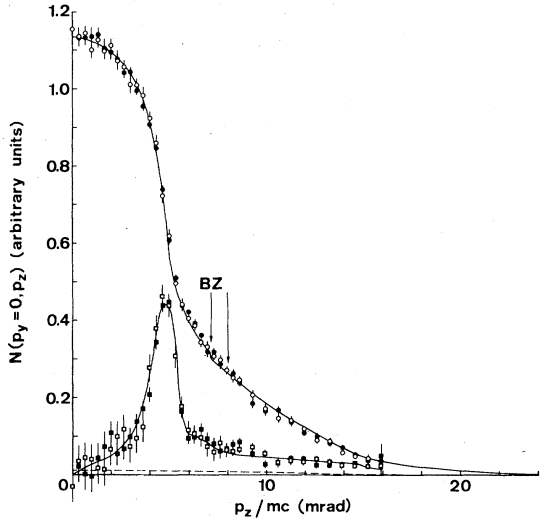

FIG. 6. As Fig. 4, but for orientation C ($\{p_z,p_x\}=\{[101],[10\bar{1}]\}$).

below). We note a reduction in $\hat{\sigma}$ from ~30 to 80 for the case of no enhancement, no core reduction, to ~2.5 to 16 for enhancement according to Eq. (6), and a core fraction of 0.2.

Folding of the angular correlation curves with the p_y resolution is essential to obtain a good fit (cf. rows 3, 5, and 6). Performing this folding by means of five- instead of three-point Gaussian quadrature improves the fits for two of the orientations (A and C, cf. rows 5 and 6).

As already mentioned, the FS resulting from the calculation is slightly less anisotropic than the experimental FS of Halse. This could affect the angular correlation curves, especially at values

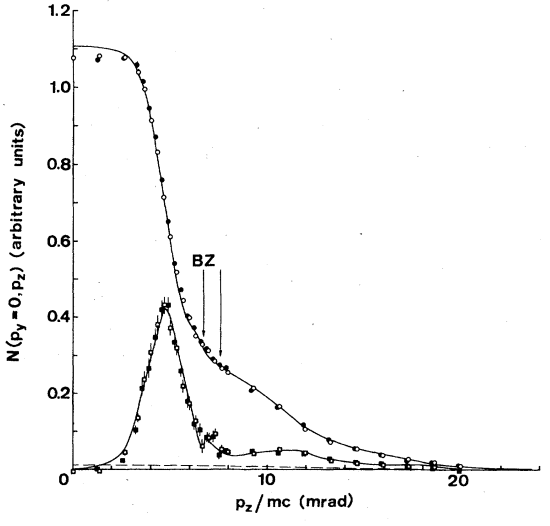

FIG. 5. As Fig. 4, but for orientation B ($\{p_z,p_x\}=\{[001],[110]\}$).

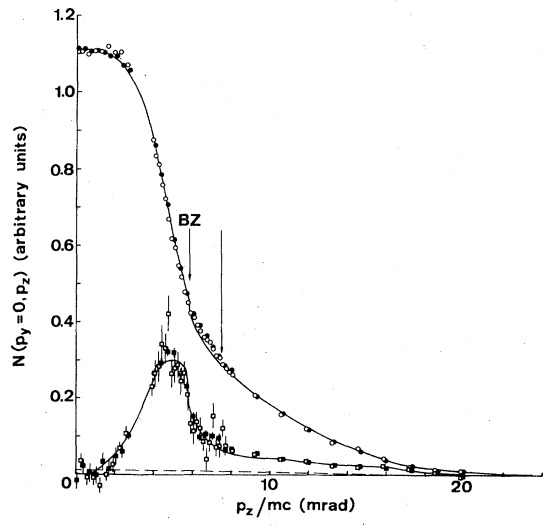

FIG. 7. As Fig. 4, but for orientation D ($\{p_z,p_x\}=\{[111],[\bar{1}10]\}$).

of p_z for which the line of integration intersects the FS under an oblique angle. The influence of this was checked by replacing the positions of the Fermi breaks in $\rho(\vec{p})$ by those derived from the Halse surface. The results appear hardly sensitive to this change (cf. rows 4 and 6).

The adjustment of the core fraction α has a large effect on the quality of the fits. Row 6 of Table III shows that the minima of $\hat{\sigma}$ fall at values of α between 0.2–0.4. However, if the experimental points just beyond the zone boundary are omitted from the fit (a procedure that will be justified below) the minima in $\hat{\sigma}$ are lowered and shifted towards a lower α, as shown by the last row of Table III. The values of α obtained in this way are, respectively, 0.18 (A), 0.20 (C and D), and 0.33 (B). Apart from the last one, they all cluster around the same number. Thus if the last result is ignored for the moment it can be concluded that the core contribution in Cu should be given a weight of ~0.20 with respect to the band electrons. This reduction by a factor of ~5 is considerably larger than the factor of 2 found by Mader *et al.*[13] in Al and will be discussed in Sec. IV.

The resulting angular correlation curves [with $\alpha = 0.20$, enhancement according to Eq. (6), correction for instrumental resolution, and use of the experimental Fermi surface of Halse] are shown in Figs. 4–7, together with their derivatives. On the whole, the agreement with the experimental data is excellent, especially if it is remembered that α is the only fitting parameter. The most notable difference is found in curve B (Fig. 5) between 0 and 2 mrad. The reason for this discrepancy is not clear, but it probably explains why for this orientation $\hat{\sigma}$ reaches its minimum at a higher fraction α than for the other orientations. On the other hand, even the small shoulders at ~7 mrad in the derivative curves for orientations A and B are accurately reproduced. For orientation B these shoulders, together with the broad shoulder at 11.5 mrad in the derivative curve and the bulge between ~8 and ~12 mrad in the angular correlation curve, are all caused by the onset of the umklapp contributions centered at (002), (222), (442), etc., followed by a lining up of the necks and the cutoff of the umklapp contributions centered around (111), (331), etc. The little shoulder observed for A, together with the faint bulge around ~9 mrad in the angular correlation, both originate in the onset of the (002), (202), etc., umklapp contributions.

A feature common to all calculated curves is the small discontinuity at the zone boundary. It is caused by the restriction of the enhancement [Eq. (6)] to states in the first zone, which makes ϵ' drop discontinuously at the zone face to its value $\epsilon'(\Gamma_1)$. The experimental points suggest that such a discontinuity does not exist and that the umklapp momentum density in the next zone is likewise enhanced. However, the enhancement factor decreases rapidly to its constant value $\epsilon'(\Gamma_1)$ as one moves away from the zone face. This is particularly clear in the case of orientation D where scanning along the [111] direction allows observation of the neck of the FS free from interference by the bulk of the FS. Up to the intersection with the hexagonal zone face at 5.81 mrad the calculated curve follows the data points closely, but between 5.81 and 7.4 mrad the latter lie above the curve. For the other orientations this effect is less pronounced since there the main contributions at the zone faces come from relatively low-lying d states. Altogether, these results agree qualitatively with the predictions of Hede and Carbotte[16] concerning the enhancement of umklapp components. There is no indication of the presence of the de-enhancement effect predicted by Fujiwara *et al.*[17] because in that case the experimental points just beyond 5.81 mrad would lie below curve D instead of above it.

Obviously, the lack of fit at points just beyond the zone boundary has an adverse effect on the goodness-of-fit parameter $\hat{\sigma}$ and obscures the excellent fit along the remainder of each curve. As already mentioned, $\hat{\sigma}$ has therefore also been calculated under exclusion of these points (over a range indicated by arrows in Figs. 4–7). The values obtained in this way are given in the last row of Table III and show the great improvement obtained especially for orientation D. For this ori-

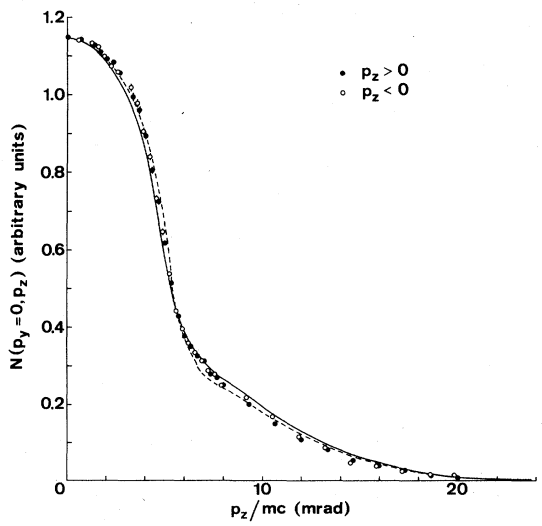

FIG. 8. Influence of enhancement and of p_y resolution correction for orientation A. Solid curve: corrected for p_y resolution, no enhancement; broken curve: enhancement correction applied, no resolution correction.

entation it also appeared necessary to change the normalization by 0.35% in order to make up for the missing area between 5.81 and 7.4 mrad.

In order to illustrate the relative importance of the enhancement and the correction for the instrumental resolution Fig. 8 shows the results for orientation A with each correction removed in turn. It is clear that the correction for enhancement is the more important one. Without it, the tail of the calculated curve is too high relative to the low-momentum part and the familiar bulge[18,19] at low momenta is absent.

2. *CuZn alloy*

Of course, the power of the positron annihilation technique does not lie in pure metals, but in disordered alloys.[2,24,41] We therefore present in Fig. 9 two-dimensional angular correlation curves for $Cu_{0.7}Zn_{0.3}$, calculated on the basis of the rigid-band model. The Fermi energy $E_F = 0.656$ Ry was obtained from the density-of-states curve. The Fermi-surface radii $k_{100} = 0.909$, $k_{110} = 0.830$, and $k_{\text{neck}} = 0.266$, all in units of $2\pi/a$, agree reasonably well with the ATA values of Bansil *et al.*[23] The curves have been enhanced following Eq. (6) with $b/a = 0.187$ and $c/a = 0.128$, values obtained from Kahana's theory by interpolation for $r_s = r_s^{Cu}/(1.3)^{1/3} = 2.45$. The same value $\alpha = 0.20$ as for pure Cu has been used, but no instrumental resolution function has been folded in. The discontinuities due to the break in the enhancement factor at the zone faces are clearly visible in all enhanced curves. In reality, however, the enhancement is expected to extend across the zone faces like in pure Cu and the discontinuities will be absent. The most striking feature is the little peak at 2.5 mrad in the curves for orientation B that is due to the contribution of the neck region. Enhancement further amplifies the peak. The curves for the other orientations are rather featureless. The difference between the enhanced and unenhanced curves is generally the same for all orientations; a bulge in the central part and a lower high-momentum part for the enhanced results. Full two-dimensional data have so far been published for an alloy with 11.6-at.% Zn,[41] and data for $Cu_{0.7}Zn_{0.3}$ will soon be available.[35]

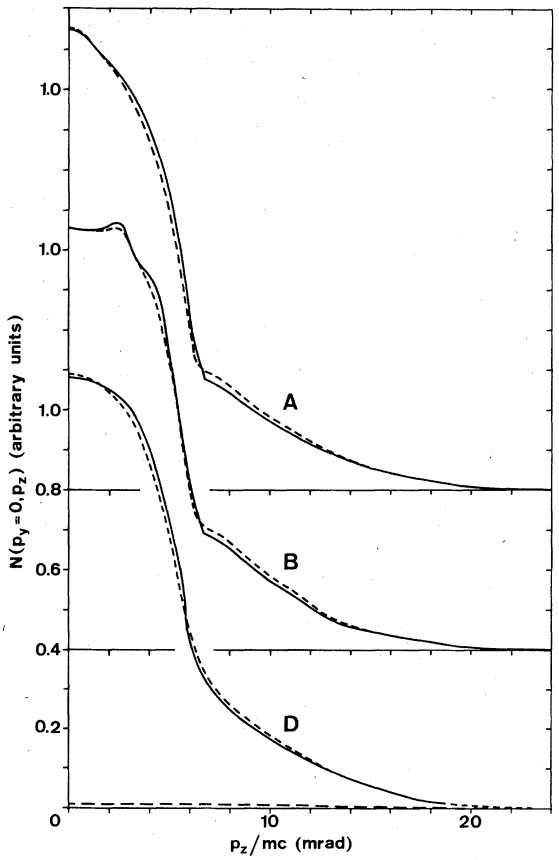

FIG. 9. Calculated point-slit angular correlation curves for $Cu_{0.7}Zn_{0.3}$ for orientations A, B, and D. Broken curves: without enhancement; solid curves: with enhancement.

IV. DISCUSSION

Visual inspection of Figs. 4–7 shows that the agreement between calculation and experiment is excellent, except perhaps for the points between 0 and 2 mrad for orientation B. Yet, considering the values of $\hat{\sigma}$ in the last row of Table III (from ~2.5 to ~16.3 for the best fits) and comparing them with the probabilities given in Sec. IID of finding a certain value of $\hat{\sigma}$ if the measured and calculated curves represent the same distribution, it is clear that the calculations are less than perfect. The remaining discrepancies are of the order of 0.5% of $N(p_z = 0)$. It is unlikely that there is one single cause for these. The 0.5% level is thought to be the level of accuracy of many parts of the calculation. To improve on this one would have to replace the Hubbard approximation scheme by a full augmented plane wave calculation and compute the eigenvalues and overlap integrals on a finer grid than that employed in the present work. Also, the convolution with the p_y resolution may have to be performed more accurately, depending on the value of the resolution. Furthermore, there is the uncertainty in the crystal potential, the exchange part should be subtracted from the positron lattice potential, and one would possibly have to consider the influence of non-muffin-tin potential terms on both the positron and electron wave functions. Finally, the core enhancement may well be somewhat momentum dependent and there may be some uncertainty in the coefficients in Eq. (6).

The residual discrepancies that prevent $\hat{\sigma}$ from reaching minimum values between ~−3.0 and +3.0 as the core fraction α is varied also cause some uncertainty in the correct value of α. This is illustrated by the decrease in the values of α that correspond to the minimum in $\hat{\sigma}$ in going from row 6 to row 7 in Table III. The present value of $\alpha \sim 0.20$ is much lower than the value of ~0.5 found in Al[13] and somewhat lower than expected. The lower density of conduction electrons in Cu results in an averaged conduction-electron enhancement $\epsilon_{\text{cond}}^{\text{Cu}} \sim 6$, i.e., 1.4 times that for Al ($\epsilon_{\text{cond}}^{\text{Al}} \sim 4.2$).[15] This ratio is not very sensitive to the exact form of the momentum dependence of ϵ_{cond}. Calculations of the core enhancement ϵ_{core} in Cu are not available, but as the binding energies of the Cu $3s$-$3p$ and the Al $2s$-$2p$ shells are about equal, it is unlikely that $\epsilon_{\text{core}}^{\text{Cu}}$ will be very different from $\epsilon_{\text{core}}^{\text{Al}}$. Thus one would expect $\alpha \sim 0.5/1.4 = 0.36$, nearly a factor of 2 larger than found in this study. According to Carbotte and Salvadori[20] $\epsilon_{\text{core}}^{\text{Al}} \sim 2.8$, whereas $\alpha \sim 0.5$, as found by Mader *et al.*,[13] together with $\epsilon_{\text{cond}}^{\text{Al}} \sim 4.2$ implies $\epsilon_{\text{core}}^{\text{Al}} \sim 2.1$. The present value of $\alpha \sim 0.20$ would mean $\epsilon_{\text{core}}^{\text{Cu}} = \alpha \epsilon_{\text{cond}}^{\text{Cu}} \sim 1.2$, significantly lower than $\epsilon_{\text{core}}^{\text{Al}}$. In this respect it is interesting to note that Lynn *et al.*[42] in their study of the core enhancement in Al have found that for momenta $\gtrsim 2p_F$ the core enhancement appears to be no more than a few tens of percent. Possibly, the introduction of a momentum-dependent core enhancement factor, decreasing for $p \gtrsim 2p_F$, could resolve this discrepancy. Besides being physically attractive (tightly bound core electrons are expected to correlate less with the positron than more loosely bound electrons) this would improve the agreement for at least two of the investigated orientations (A and C). Finally, it should not be excluded that the low value of α could (partly) be a result of the residual discrepancies mentioned at the beginning of this paragraph, and that an increased accuracy of the calculations could raise α to a value more consistent with the expected core enhancement.

In long-slit angular correlations the core contribution is much more important (as a result of the double integration) than in point-slit curves. Yet, in most calculations of long-slit curves[10-12] the core is included with unit weight. In view of the low α found in this work it is not surprising that these calculations, while able to predict the anisotropy to a high precision, always seem to overestimate the high-momentum content of the long-slit angular correlations. In fact, taking $\alpha = 1$ produces the same effect in our calculated point-slit curves.

The success of the present calculations is for a large part due to the use of the enhancement correction in the energy-dependent form Eq. (6) rather than in its more familiar momentum-dependent formulation Eq. (1). This does not mean that Eq. (6) fully describes enhancement in real metals. In particular, it does not provide the enhancement of the umklapp components which is needed to fit the experimental points at p_z values in the small interval just beyond a zone face. In spite of this, the present approach works remarkably well. If it turns out to be equally successful in other d-band metals, it might induce the many-body theorists to develop a more general description of enhancement. Until such a theory becomes available Eq. (6) may be considered as an empirical prescription for handling enhancement in copper and possibly also other d-band metals.

V. CONCLUSIONS

The present study has demonstrated that band-structure calculations are capable of predicting (point-slit) angular correlations of annihilation quanta in Cu to a high degree of accuracy. An essential ingredient of this success is the energy-dependent "Kahana enhancement" proposed in this paper in combination with a reduced core contribution. A careful comparison of theory and experiment confirms the theoretical results of Hede and Carbotte concerning the enhancement of umklapp components. No indication is found of a de-enhancement for momenta just beyond a zone face.

ACKNOWLEDGMENTS

One of us (R.M.S.) is grateful to the Alexander von Humboldt Foundation for a fellowship and to the Kernforschungsanlage Jülich, especially Professor W. Triftshäuser, for the kind hospitality extended to him. We wish to thank Professor S. Berko and Dr. J. Mader for their permission to use their experimental data prior to publication and are grateful to the former for several interesting discussions.

*Present address: Dept. of Physics, Indian Institute of Technology, Kanpur-208016, India.

[1] R. N. West, Adv. Phys. 22, 263 (1973).
[2] S. Berko and J. Mader, Appl. Phys. 5, 287 (1975).
[3] S. Berko, in *Compton Scattering*, edited by B. Williams (McGraw-Hill, London, 1977), Chap. 9; P. E. Mijnarends, in *Positrons in Solids*, edited by P. Hautojärvi (Springer-Verlag, Heidelberg, 1979), Chap. 2.
[4] R. M. Singru, Phys. Status Solidi A 30, 11 (1975).

[5]S. Berko, M. Haghgooie, and J. J. Mader, Phys. Lett. A 63, 335 (1977).
[6]A. A. Manuel, S. Samoilov, Ø. Fischer, M. Peter, and A. P. Jeavons, J. Phys. (Paris) 39, C6-1084 (1978).
[7]R. N. West (private communication).
[8]W. Triftshäuser, in *Festkörperprobleme*, edited by H. J. Queisser (Pergamon/Vieweg, Braunschweig, 1975), Vol. XV, p. 381.
[9]R. J. Douglas and A. T. Stewart, Paper H 14, Fourth International Conference on Positron Annihilation, Helsingør, 1976 (unpublished).
[10]S. Wakoh, Y. Kubo, and J. Yamashita, J. Phys. Soc. Jpn. 38, 416 (1975); N. Shiotani, T. Okada, T. Mizoguchi, and H. Sekizawa, J. Phys. Soc. Jpn. 38, 423 (1975).
[11]N. Shiotani, T. Okada, H. Sekizawa, S. Wakoh, and Y. Kubo, J. Phys. Soc. Jpn. 43, 1229 (1977).
[12]R. M. Singru and P. E. Mijnarends, Phys. Rev. B 9, 2372 (1974); R. M. Singru, Pramāna 2, 299 (1974).
[13]J. Mader, S. Berko, H. Krakauer, and A. Bansil, Phys. Rev. Lett. 37, 1232 (1976).
[14]Atomic units with $\hbar = m = e = 1$ and $c = 137$ are used throughout, but energies are measured in Ry.
[15]S. Kahana, Phys. Rev. 129, 1622 (1963); J. P. Carbotte and S. Kahana, *ibid.* 139, A213 (1965); J. P. Carbotte, *ibid.* 155, 197 (1967).
[16]B. B. J. Hede and J. P. Carbotte, J. Phys. Chem. Solids 33, 727 (1972).
[17]K. Fujiwara, J. Phys. Soc. Jpn. 29, 1479 (1970); K. Fujiwara, T. Hyodo, and J. Ohyama, *ibid.* 33, 1047 (1972); K. Fujiwara and T. Hyodo, *ibid.* 35, 1664 (1973).
[18]J. J. Donaghy and A. T. Stewart, Phys. Rev. 164, 396 (1967).
[19]J. Melngailis and S. DeBenedetti, Phys. Rev. 145, 400 (1966).
[20]J. P. Carbotte and A. Salvadori, Phys. Rev. 162, 290 (1967).
[21]J. Mader, Ph.D. thesis (Brandeis University, 1975) (unpublished).
[22]See also, full surfaces for Cu in M. Haghgooie, J. J. Mader, and S. Berko, Phys. Lett. A 69, 293 (1978).
[23]A. Bansil, H. Ehrenreich, L. Schwartz, and R. E. Watson, Phys. Rev. B 9, 445 (1974).
[24]S. Berko and J. Mader, Phys. Condens. Matter 19, 405 (1975); W. Triftshäuser and A. T. Stewart, J. Phys. Chem. Solids 32, 2717 (1971); E. H. Becker, P. Petijevich, and D. Ll. Williams, J. Phys. F 1, 806 (1971).
[25]D. G. Kanhere and R. M. Singru, J. Phys. F 7, 2603 (1977).
[26]Recent ATA calculations of the momentum density for Compton scattering in disordered alloys by Mijnarends and Bansil [Phys. Rev. B 13, 2381 (1976), and *ibid.* (to be published)] do not include the positron and therefore do not describe e^+ distribution and e^+ disorder scattering effects (Ref. 27).
[27]K. M. Hong and J. P. Carbotte, Can. J. Phys. 55, 1335 (1977).
[28]G. A. Burdick, Phys. Rev. 129, 138 (1963).
[29]J. Hubbard, J. Phys. C 2, 1222 (1969); J. Hubbard and P. E. Mijnarends, *ibid.* 5, 2323 (1972).
[30]P. E. Mijnarends, Physica (Utr.) 63, 235 (1973).
[31]A. G. Gould, R. N. West, and B. G. Hogg, Can. J. Phys. 50, 2294 (1972).
[32]F. Herman and S. Skillman, *Atomic Structure Calculations* (Prentice-Hall, Englewood Cliffs, 1963).
[33]A. Ralston, *A First Course in Numerical Analysis* (McGraw-Hill-Kogakusha, Tokyo, 1965), Chap. 6, p. 240.
[34]For orientation *C* (see Table I) a fit to seven points was used in view of the lower statistical accuracy of the experimental data.
[35]S. Berko (private communication).
[36]Ref. 33, p. 97.
[37]With $a = 1$, $b/a = 0.195$, and $c/a = 0.138$.
[38]I. Epstein and B. Williams, Philos. Mag. 27, 311 (1973).
[39]M. R. Halse, Philos. Trans. R. Soc. A 265, 507 (1969).
[40]1 unit of $mc \times 10^{-3}$ is equivalent to 0.137 a.u. or to an angular deviation of 1 mrad between the annihilation quanta.
[41]S. Berko, M. Haghgooie, and J. J. Mader, in *Transition Metals*, Institute of Physics Conference Series No. 39 (Institute of Physics, Bristol, 1978), p. 94.
[42]K. G. Lynn, J. R. MacDonald, R. A. Boie, L. C. Feldman, J. D. Gabbe, M. F. Robbins, E. Bonderup, and J. Golovchenko, Phys. Rev. Lett. 38, 241 (1977).